Evaluation of metabolic changes in liver and serum of streptozotocin-induced diabetic rats after Mango diet supplementation

Álvaro Fernández-Ochoa[a,b,1], Rosario Cázares-Camacho[c,1], Isabel Borrás-Linares[b], J. Abraham Domínguez-Avila[d], Antonio Segura-Carretero[a,b,2,*], Gustavo Adolfo González-Aguilar[c,2]

[a] Department of Analytical Chemistry, Faculty of Sciences, University of Granada, Av Fuentenueva s/n, Granada 18071, Spain
[b] Research and Development of Functional Food Centre (CIDAF), Health Science Technological Park, Av del Conocimiento, n° 37, Granada 18016, Spain
[c] Coordinación de Tecnología de Alimentos de Origen Vegetal, Centro de Investigación en Alimentación y Desarrollo A.C. (CIAD), Carretera Gustavo Enrique Astiazarán Rosas No. 46, Hermosillo 83304, Mexico
[d] Cátedras CONACYT-Coordinación de Tecnología de Alimentos de Origen Vegetal, Centro de Investigación en Alimentación y Desarrollo A.C. (CIAD), Carretera Gustavo Enrique Astiazarán Rosas No. 46, Hermosillo 83304, Mexico

ARTICLE INFO

ABSTRACT

Mango consumption has shown bioactive properties against several diseases like diabetes, therefore, we evaluated how a mango-supplemented diet affects metabolic pathways in diabetic rats. Serum and liver samples were collected from 26 rats divided into 3 groups (healthy, untreated diabetic and mango-treated diabetic) after dietary intervention and analysed using an LC-MS untargeted metabolomic strategy. Twenty-six and 29 metabolites in serum and liver were potentially annotated, showing significant differences among groups. Several affected pathways were due to the disease state [fatty acids (i.e. palmitoleic, linolenic, stearidonic, eicosapentaenoic, docosahexaenoic acids and others), bile acids (i.e. glycocholic acid) and amino acids (i.e. leucine, isoleucine and valine)], and others due to mango supplementation (increased hepatic bioaccumulation of euxanthone, a mangiferin metabolite, and increased glutathione concentration). These results suggest that a mango-supplemented diet exerted a significant antioxidant effect in the liver of diabetic rats, likely due to its phenolic compounds, like mangiferin and its metabolites.

1. Introduction

Diabetes mellitus (DM) is among the most prevalent chronic diseases in the world, as stated by the International Diabetes Federation (IDF). In 2017, there were approximately 451 million diagnosed patients and 5 million deaths worldwide were related to DM (Cho et al., 2018). DM alludes to a group of metabolic disorders characterized by chronic hyperglycemia, resulting from impaired insulin production by pancreatic β-cells and/or insulin resistance by peripheral tissues (Goyal & Jialal, 2018). Genetic, environmental and lifestyle (diet and exercise) factors are among the different causes that can promote or prevent DM development. Moreover, oxidative stress has been strongly associated with DM pathogenesis and the progression of its comorbidities.

Recent studies have reported that vegetable byproducts, which are often discarded in industrial processing (e.g. bark, peel, leaves, roots, seeds, flowers, etc.), are potential sources of bioactive compounds that can exert antidiabetic and antioxidant actions, similar to those of commercially-available drugs (Naveen & Baskaran, 2018). Fenugreek, avocado, garlic, pomegranate, grapes, guava and papaya are crops whose bioactive components have been extensively studied as antidiabetics, mainly due to their powerful antioxidant activity and hypoglycemic effects, as proven in animal models and clinical trials (Beidokhti & Jäger, 2017; Naveen & Baskaran, 2018). Among them, mango (Mangifera indica L.) cv. 'Ataulfo' is an excellent source of nutritional (vitamins, minerals, dietary fiber) and bioactive compounds (carotenoids and phenolic compounds) with functional properties (Palafox-Carlos, Yahia, & González-Aguilar, 2012).

Mango consumption, or that of its main bioactive compounds, has

---

been linked to antimutagenic, anti-inflammatory, immunomodulatory, antioxidant, hypoglycemic and antidiabetic effects (Martin & He, 2009; Velderrain-Rodríguez et al., 2018). Previous studies have been carried out to validate the effectiveness of consuming mango peel extract to modulate oxidative stress and ameliorate various biochemical parameters in streptozotocin (STZ)-induced diabetic rats. Numerous mechanisms of action have been proposed to explain the effects observed, for example, improving serum glucose uptake and catabolism, increasing antioxidant system activity and inhibiting digestive starch-hydrolyzing enzymes, among others (Gandhi et al., 2014; Gondi & Rao, 2015; Sellamuthu, Arulselvan, Muniappan, Fakurazi, & Kandasamy, 2013).

There is substantial evidence correlating diabetic complications to disrupted common metabolic pathways. In this way, different metabolites, such as some lipids, monosaccharides and amino acids have been identified as altered in individuals with DM (Sas, Karnovsky, Michailidis, & Pennathur, 2015). Having a thorough knowledge of how these metabolites change in response to the disease and/or dietary patterns, could be used as promising biomarkers that could lead to improving early diagnosis, generate novel and effective treatments and propose personalized dietary recommendations. These molecules have been identified thanks to the recent development of metabolomic approaches, which aim to study a substantial number of low-molecular-weight compounds present in biological systems (Agin et al., 2016). Human clinical trials provide promising results but are not always consistent, they have some limitations like elevated costs, duration of the studies, sample size and high biological variability (Szkudelski & Szkudelska, 2015). In the field of DM research, several animal models have been developed to elucidate the mechanisms and metabolic alterations underlying DM and its comorbidities (King & Bowe, 2016). STZ-induced diabetic rat models are widely used to evaluate metabolic profiles (Chen et al., 2011), having some advantages such as standardized protocols, quick onset of the disease, less expensive and faster than others. In contrast, STZ-induced diabetes does not reflect the full course of disease in humans, who usually develop after years of asymptomatic metabolic alterations, beginning with insulin resistance, progressing to impaired glucose metabolism and finally to DM. Nonetheless, preclinical trials in animal models remain as the most viable alternative for a better understanding of the disease and improving the predictably of results in the discovery of new therapeutic agents for human application.

Due to the promising beneficial effects of mango consumption in DM, the aim of the present study was to evaluate metabolic changes in serum and liver of STZ-induced diabetic Wistar rats, after prolonged intake of bioactive compounds from 'Ataulfo' mango peel and pulp. Our data will contribute to identifying potential changes to diabetes-related biomarkers after consumption of a mango-supplemented diet rich in bioactive compounds.

2. Material and methods

2.1. Animals and samples

All experiments involving living organisms were reviewed and approved by the Bioethics Committee of the Research Center for Food and Development, where they were performed (CE/013/2018). Animals were cared for and manipulated according to applicable local and international rules and regulations, such as the Guide for the Care and Use of Laboratory Animals of the National Institutes of Health and the Mexican NOM-062-ZOO-1999. Twenty-six male Wistar rats (280 ± 40 g initial weight) were obtained from the University of Sonora, Mexico, and housed in individually ventilated metal cages under standard conditions (12 h light/dark cycles at 24 ± 1 °C). After seven days of acclimatization with free access to food and water, rats were randomly divided into three groups: healthy control group (HC, n = 7), untreated diabetic group (UD, n = 6) and mango-treated

diabetic group (MTD, n = 13). Diabetes was induced on UD and MTD groups under overnight fasted conditions by an intraperitoneal dose of STZ (60 mg/kg body weight) dissolved in 0.9% NaCl. Three days after the STZ dose, blood samples were taken from the tail vein, and glucose concentration was measured with a commercial glucose meter. Rats with glycemia ≥ 200 mg/dL were considered diabetic and used for the experiment. Initial and final glycemia and body weight gain were registered (Table S1).

HC and UD groups were fed a diet based on the standard A5001 diet; after diabetes was confirmed, the MTD group was immediately fed with a diet supplemented with 5% and 10% lyophilized 'Ataulfo' mango peel and pulp, respectively. Diets were isoenergetic (3.5 kcal/g), with a macro- and micronutrient content adequate for rodents (Table S2). The phytochemical content of mango peel and pulp has been reported in previous papers (see Supplemental Material) (Pacheco-Ordaz, Antunes-Ricardo, Gutiérrez-Uribe, & González-Aguilar, 2018; Quirós-Sauceda et al., 2017; Velderrain-Rodríguez et al., 2018).

The different diets were consumed by the animals for 5 weeks, during which food and water were freely available and replenished daily. After that period, they were fasted overnight (10 h), anesthetized with a single intraperitoneal dose of sodium pentobarbital (120 mg/kg body weight; Pisabental, PISA Agropecuaria, Atitalaquia, Hidalgo, Mexico) and euthanized. Whole blood samples were collected in gold-top serum separator Vacutainer tubes (Becton-Dickinson, Franklin Lakes, NJ, USA) to obtain serum, while liver samples (0.5 g) were lyophilized. Both types of samples were stored at −80 °C until processed.

2.2. Sample treatment

Biological samples were thawed on ice before analysis. A quality control sample (QC) was prepared for each matrix by combining equal amounts of each case-study sample. This QC sample was treated like the study samples as described below.

In the case of serum samples, a mixture of organic solvents (methanol:ethanol, 50:50 v/v) was used for protein removal. The mixture was kept for 30 min at −20 °C and then centrifuged (14,800 rpm, 4 °C, 10 min). The supernatant (200 μL) was evaporated to dryness. After solvent evaporation, the dry residue was reconstituted in 100 μL of H_2O:methanol: (95:5, v/v) and centrifuged to collect an aliquot for HPLC-MS analysis.

Regarding liver samples, 100 mg of lyophilized tissue were weighed and mixed with 500 μL of methanol. Before LC-MS analysis, the metabolites and proteins were extracted and removed, respectively. For that, the mixture was vortex-mixed and then introduced into an ultrasonic bath for 3 min under refrigerated conditions. The mixture was kept for 30 min at −20 °C and then centrifuged (14,800 rpm, 4 °C, 10 min). The supernatant was separated, and the extraction process was repeated two more times using 250 μL of methanol:H_2O (80:20, v/v). The use of 100% or 80% methanol allows a better extraction of metabolites and, therefore, thus a greater coverage of the metabolome (Wells et al., 2018). The supernatants were mixed, and a 700 μL aliquot was evaporated to dryness. Finally, the residue was reconstituted in 150 μL of methanol:H_2O (35:65, v/v), taking an aliquot for HPLC-MS.

2.3. HPLC-MS analysis.

Both biological samples were analyzed with the same HPLC-ESI-QTOF-MS methodology. Metabolites were separated using an Agilent Zorbax Eclipse Plus column (3.5 μm particle size, 150 mm × 2.1 mm). The column was maintained at 25 °C in an Agilent 1260 HPLC instrument. Mobile phases were water (A) and methanol (B), both containing 0.1% formic acid. These were used with a flow rate of 0.4 mL/min with the following gradient: 0 min, 5% B; 5 min, 10% B; 15 min, 85% B; 32–40 min, 100% B; 45–50 min, 5% B. Injection volume was 5 μL, and for avoiding possible degradation, samples were maintained at 4 °C in
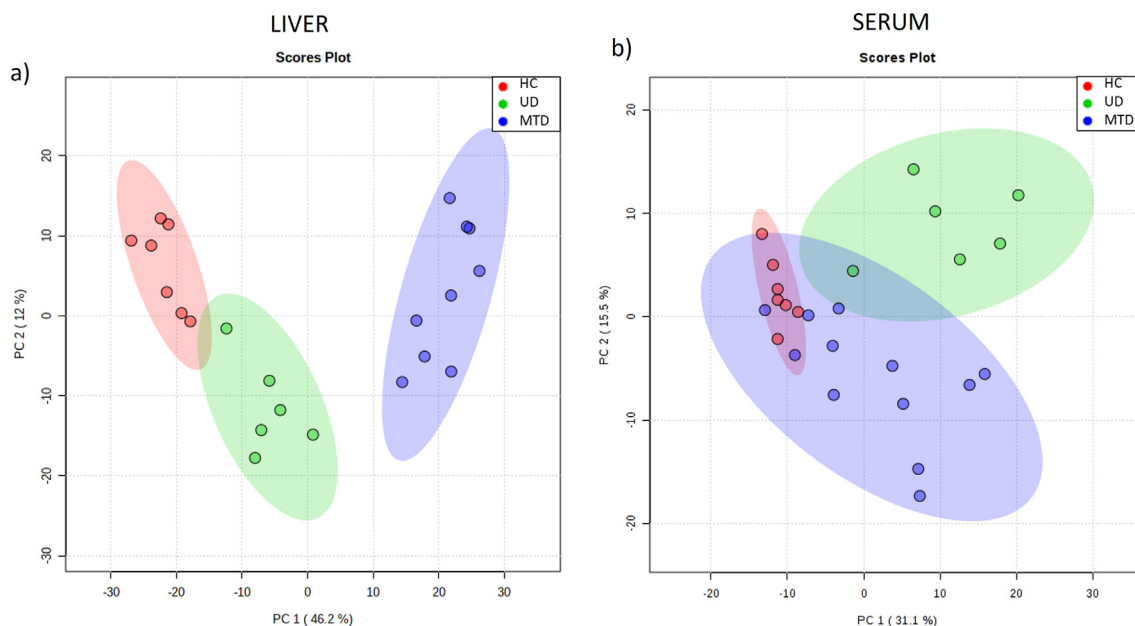
Fig. 1. PCA scores plots from data obtained in the analyses from liver (a) and serum samples (b) after the removal of outliers and QC samples. (Red dots, healthy controls, HC; green dots, untreated diabetic group, UD; blue dots, mango-treated diabetic group, MTD). (For interpretation of the references to colour in this figure legend, the reader is referred to the web version of this article.)

the auto-sampler compartment. The QC sample and an analytical blank were repeatedly injected every five study samples throughout the analytical sequence. Study samples were randomly injected into the analytical sequence in order to avoid the risk of false positive and carrier effects.

MS analyses were performed using an Agilent 6540 UHD Accurate Mass Q-TOF analyzer. Data was acquired in negative-ion mode over a 50 to 1700 m/z range. For identification purposes, MS/MS analyses were performed in QC samples with different collision energies (10, 20 and 40 eV). Ultrahigh purity nitrogen was used as drying (200 °C, 10 L/min) and nebulizer gas (350 °C, 12 L/min). All masses were calibrated by means of continuous infusion of the following substances: tri-fluoroacetate anion ($C_2F_3O_2^-$, m/z 112.985587) and an adduct of HP-921 (m/z 1033.988109). Both reference ions provided accurate mass measurements, typically better than 2 ppm. The analytical methodology is described in detail elsewhere (Fernández-Ochoa et al., 2019).

2.4. Data processing and statistical analysis

Batch Recursive Feature Extraction for small molecules was performed using MassHunter Profinder software (B.06.00, Agilent Technologies). Parameters for peak picking were an intensity threshold of 1000 counts, an RT window of ± 0.25 min, a mass window of 20 ppm ± 2 mDa and Agile2 as the integration method. Possible adducts with a maximum charge of 2 were the following: $[M-H]^-$, $[M+Cl]^-$, $[M-H_2O-H]^-$ and $[M+HCOO]^-$.

Regarding statistical analyses, Principal Component Analysis (PCA) was performed first to check the reproducibility and detect possible outliers. In order to explore the metabolic differences in relation to the different study groups, multivariate statistical test (Partial Least Squares Discriminant Analysis (PLS-DA), and a hierarchical clustering via heatmap) and univariate statistical tests (ANOVA) were performed. Logarithmic transformation and Pareto scaling were applied to the data before performing multivariate analyses. All statistical tests were carried out in MetaboAnalyst 4.0 software (Chong et al., 2018). Molecular features with VIP values higher than 1.50 in PLS-DA models were selected for identification as potential biomarkers. Furthermore, analysis of variance (ANOVA) was applied to these features, and those that were not significant in this statistical test (p-value > 0.05) were discarded

for identification.

2.5. Metabolite identification

Identification of the selected molecular features in statistical tests was carried out by comparing accurate mass, isotopic distribution and fragmentation patterns obtained in MS/MS analysis with available on-line metabolomic databases. Databases were searched by CEU Mass Mediator tool (Gil de la Fuente, Grace Armitage, Otero, Barbas, & Godzien, 2017). This tool allowed simultaneous metabolite search in several databases such as METLIN, LipidMaps, KEGG as well as Human Metabolome Database. The MS/MS patterns were also compared with *in silico* MS/MS fragmentation resources, concretely, MetFrag (https://ipb-halle.github.io/MetFrag/).

3. Results

3.1. Data quality assessment

After data pre-processing, 770 and 508 molecular features were extracted from liver and serum samples, respectively. After that, 19 and 32 features were discarded from both datasets, respectively, due to a Relative Standard Deviation (RSD) in QC samples higher than 30%. PCA was performed to detect outliers and check analytical reproducibility (Ulaszewska et al., 2019). In this sense, a well grouping of the QC samples in the PCA scores plot (see Fig. S1, supplemental material) indicated a good reproducibility of the obtained data. However, the first main component (PC1) of both models explained great differences between specific samples (one serum and three liver samples) and the rest of the samples. This fact implied that the separated samples were assigned as outliers, and, therefore, were discarded for the rest of the statistical analyses. Despite this, differences between groups (HC, UD and MTD) were detected thanks to the information explained by the second component (PC2) in both PCA analyses. These groupings were more clearly observed in the PCA of the liver samples. Therefore, PCA analyses were performed again without the outliers and QC samples (Fig. 1). As mentioned above, higher differences among HC, UD and MTD groups were observed in the case of liver samples. The variability explained by PC1 (46.2%) showed a clear separation among all groups
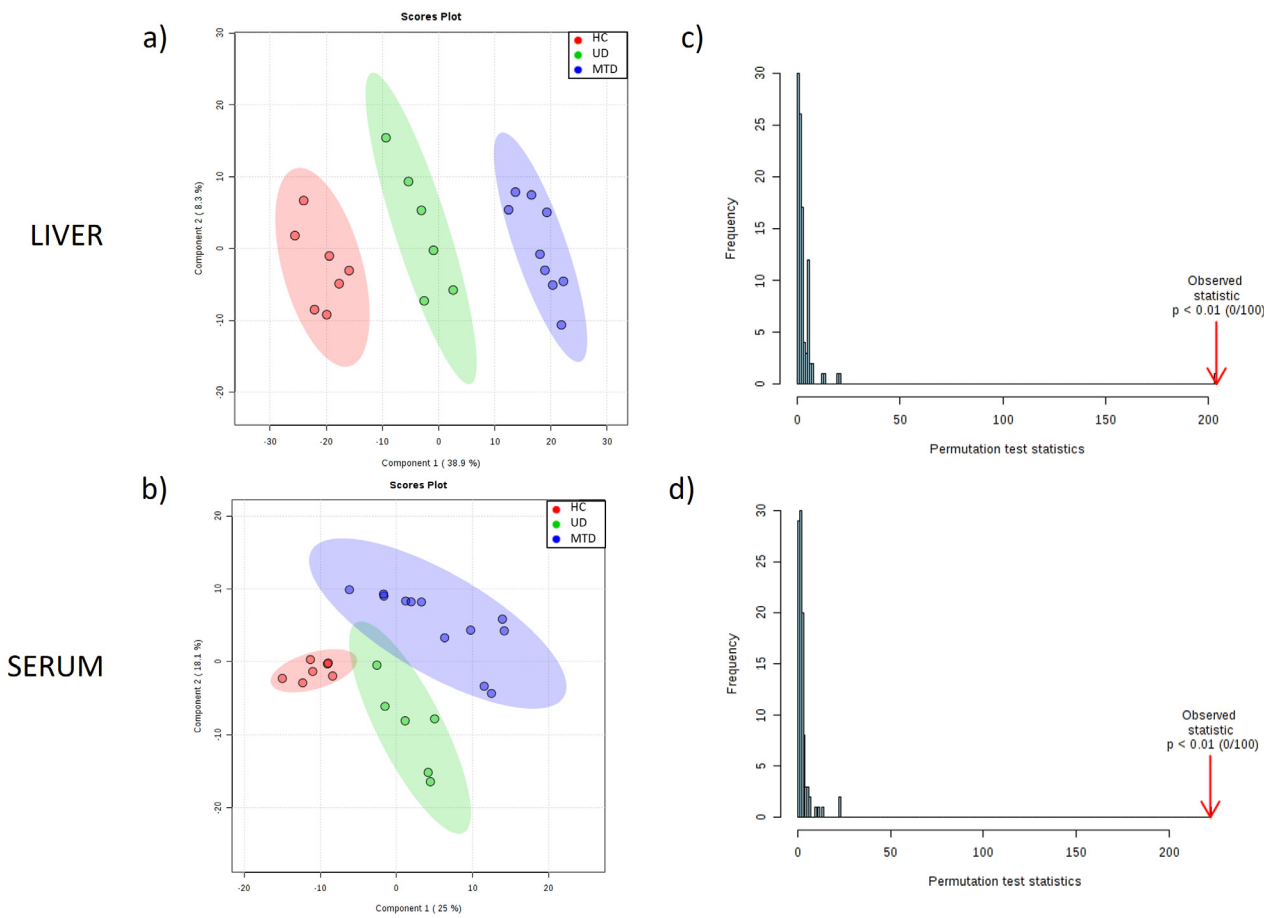
Fig. 2. A Supervised Partial Least Squares Discriminant Analyses (PLS-DA). (a, b): PLS-DA score plot (a: liver model; b: serum model). (Red dots, healthy controls, HC; green dots, untreated diabetic group, UD; blue dots, mango-treated diabetic group, MTD). Permutation test results using separation distance (B/W) (c: liver model, d: serum model). (For interpretation of the references to colour in this figure legend, the reader is referred to the web version of this article.)

(Fig. 1a). Regarding serum samples, no clear separations among the three groups were observed, as in the case of liver samples, however, a clear separation between diabetic and healthy rats was detected, as well as a good grouping of the HC samples (Fig. 1b).

3.2. PLS-DA models and analysis of variance (ANOVA)

PLS-DA models were built to discriminate samples according to different classes (HC, UD and MTD). Fig. 2 shows the main results of both models. Analogous to PCA results, the three classes were better separated by the PLS-DA model created with liver data. Clearly, all three classes were separated by PC1 (38.9%) in the PLS-DA model. On the other hand, PC1 (25%) in the model created with serum data separated the healthy controls and diabetic samples. In addition, PC2 (18.1%) differentiated rats from the UD group, to those that consumed mango-supplemented diets (MTD).

For model assessment, accuracy, R^2 and Q^2 values were obtained by 10-fold cross validation (CV) method for the PLS-DA models with two components. Analogous to the sample distribution observed in score plots, better results were obtained with the model created with liver data (Accuracy: 0.95, R^2: 0.98 and Q^2: 0.95), as compared to the model with serum data (Accuracy: 0.92, R^2: 0.84 and Q^2: 0.64). Permutation tests were also performed, in which p-values lower than 0.01 were obtained from both models (Fig. 2c, d), indicating a lack of overfitting in these models. After PLS-DA and ANOVA, 51 and 39 molecular features from liver and serum, respectively, were selected for identification. Then, 26 and 29 metabolites for serum and liver, respectively, could be annotated (Tables 1 and 2). According to the Metabolomics Standards Initiative (MSI), proposed metabolites were putatively

annotated (Sumner et al., 2007) using the MS/MS fragments (Tables S3–S4). Regarding unknown features, Tables S5–S6 show their corresponding parameters.

3.3. Hierarchical clustering analysis via heatmap

Hierarchical clustering analyses via heatmap were performed to the annotated metabolites using a Pearson distance measure and Ward clustering algorithm. Fig. 3 shows results obtained for these analyses. In both models, sample clustering shows three clear clusters (S1, S2 and S3), related to the three classes of samples (MTD, HC and UD), respectively. Regarding variable clustering, different clusters were clearly established. In liver model, four clusters (L1, L2, L3 and L4) were assigned (Fig. 3a). L1 and L2 clusters were clearly influenced by the mango-supplemented diet, while L3 and L4 seemed to be more related to diabetes. Regarding serum clustering (Fig. 3b), three clusters were established (P1, P2 and P3). The first two were made up of altered by diet, while the third cluster corresponded to metabolites influenced by diabetes.

4. Discussion

A detailed understanding of the pathophysiology of DM by identifying its metabolic alterations is imperative for early diagnosis and the development of possible preventive strategies and effective treatments. In the present study, we attempted to inspect the metabolic profile of serum and liver of STZ-induced diabetic rats using HPLC-ESI-QTOF-MS, and explore the alterations generated by a mango-supplemented diet. The most affected pathways by the pathology were related to fatty acid

Table 1
Retention times, masses, VIP, FDR and the results of the Tukey's HSD from annotated metabolites present in serum samples.

| RT (min)	Mass (Da)	VIP value	FDR	Tukey's HSD	Molecular Formula	Score (%)	Metabolite
22.58	302.2258	3.86	2.85E−08	T-C; T-D	$C_{20}H_{30}O_2$	97.82	Eicosapentanoic acid (EPA)
19.19	318.2227	3.56	2.57E−08	T-C; T-D	$C_{20}H_{30}O_3$	95.54	12-HEPE
17.95	465.3130	3.16	5.76E−03	D-C; T-C	$C_{26}H_{43}NO_6$	97.27	Glycocholic acid
1.5	270.0931	2.93	9.12E−07	D-C; T-C	$C_{10}H_{14}N_4O_5$	87.3	Histidinyl-Aspartate (His-Asp)
17.71	408.294	2.62	3.19E−02	T-C	$C_{24}H_{40}O_5$	76.36	Cholic acid
1.42	279.1320	2.56	2.69E−03	D-C; T-C	$C_{11}H_{21}NO_7$	58.12	N-(1-Deoxy-1-fructosyl)valine
24.58	330.2550	2.55	3.77E−07	T-C; T-D	$C_{22}H_{34}O_2$	97.93	Docosapentaenoic acid (DPA)
12.71	284.0918	2.55	2.52E−02	T-C	$C_{13}H_{16}O_7$	91.16	p-Cresol glucuronide
23.71	678.4681	2.28	1.80E−05	D-C; T-C; T-D	$C_{39}H_{67}O_7P$	87.31	PA(P-36:5)
12.01	86.0735	2.13	3.86E−04	D-C; T-C	$C_5H_{10}O$	85.06	Iso-valeraldehyde
6.79	118.1311	2.05	6.05E−04	D-C; T-C	$C_5H_{10}O_3$	84.99	3-hydroxyisovaleric acid
23.13	254.2265	2.05	4.81E−03	D-C; T-C	$C_{16}H_{30}O_2$	98.52	Palmitoleic acid
23.14	276.4137	2.02	3.93E−03	D-C; T-C	$C_{18}H_{28}O_2$	80.27	Stearidonic acid
34.7	583.5189	1.94	1.65E−04	D-C; T-C	$C_{34}H_{67}NO_3$	78.75	Cer(d18:1/16:0)
11.37	122.0373	1.91	5.77E−03	D-C; T-C	$C_7H_6O_2$	98.88	4-Hydroxybenzaldehyde
25.99	332.2735	1.87	8.95E−04	T-C; T-D	$C_{22}H_{36}O_2$	72.81	Adrenic Acid
1.51	129.0406	1.87	3.00E−03	T-C; T-D	$C_5H_7NO_3$	87.4	Pyroglutamic acid
23.7	396.2277	1.84	1.13E−06	T-C; T-D	$C_{18}H_{37}O_7P$	94.52	PA(15:0)
1.76	129.0419	1.83	4.66E−04	D-C; T-C	$C_5H_7NO_3$	93.43	Pyrrolidonecarboxylic acid
23.71	396.2320	1.77	1.13E−06	D-C; T-C; T-D	$C_{18}H_{37}O_7P$	99.21	(9S,10S)-10-hydroxy-9-(phosphonooxy)octadecanoate
23.72	328.2431	1.77	3.13E−06	D-C; T-C; T-D	$C_{22}H_{32}O_2$	96.02	Docosahexaenoic acid (DHA)
22.7	300.4351	1.71	2.14E−02	T-C	$C_{20}H_{28}O_2$	65.90	Retinoic acid
12.79	173.1054	1.65	4.07E−02	T-C	$C_8H_{15}NO_3$	84.38	Hexanoylglycine
22.71	278.2261	1.57	2.56E−02	T-C	$C_{18}H_{30}O_2$	76.03	Linolenic acid
21.17	567.3359	1.54	4.81E−03	D-C; T-C	$C_{30}H_{50}NO_7P$	92.64	LysoPC(22:6)
23.78	654.4694	1.53	1.11E−04	T-C; T-D	$C_{44}H_{62}O_4$	72.04	14-DHAHDHA

metabolism, bile acid homeostasis and amino acid catabolism, while metabolites enhanced by the mango treatment were associated with the antioxidant system. The following section discusses what metabolomic changes were documented, as well as their implications; they were grouped according to changes that were due to mango supplementation (4.1) and those of the disease itself (4.2).

4.1. Metabolic changes related to molecular mechanisms in response to mango-supplemented diet

The effects of mango peel and pulp intake on the serum and liver metabolome in STZ-induced rats were studied. The major findings associated with diet consumption were the presence of euxanthone and glutathione, molecules that are related to the enhancement of the antioxidant status of the liver of diabetic rats, among other biological properties, which are discussed in further detail below.

Table 2
Retention times, masses, VIP, FDR and the results of the Tukey's HSD from annotated metabolites present in liver samples.

RT (min)	Mass (Da)	VIP value	FDR	Tukey's HSD	Molecular Formula	Score (%)	Metabolite
7.61	358.1014	3.54	1.04E−10	T-C, T-D	$C_{11}H_{23}N_2O_7PS$	91.76	Pantetheine 4″-phosphate
17.34	228.0429	3.53	5.00E−17	T-C, T-D	$C_{13}H_8O_4$	95.11	Euxanthone
34.15	825.5523	3.38	6.74E−25	T-C, T-D	$C_{45}H_{80}NO_{10}P$	96.77	PS(39:4)
15.79	320.1476	3.35	3.26E−07	D-C, T-C	$C_{14}H_{28}O_8$	97.85	Octanoylglucoronide
1.47	345.0379	3.24	2.23E−16	T-C, T-D	$C_{10}H_{12}N_5O_7P$	53.27	Cyclic GMP
1.47	307.0847	3.21	1.56E−06	T-C, T-D	$C_{10}H_{17}N_3O_6S$	92.63	Glutathione
3.05	216.1133	1.68	3.04E−07	D-C, T-C, T-D	$C_9H_{16}N_2O_4$	86.73	Pro-Thr
7.25	282.1076	1.64	1.58E−09	D-C, T-C, T-D	$C_{10}H_{14}N_6O_4$	88.44	2-Aminoadenosine
2.75	176.0691	1.59	1.88E−06	D-C, T-C, T-D	$C_7H_{12}O_5$	78.56	2-Isopropylmalic acid
27.94	676.5406	1.57	7.57E−07	D-C, T-C, T-D	$C_{38}H_{77}O_7P$	97.54	PA(O-18:0/17:0)
1.41	347.0596	1.57	3.45E−08	D-C, T-C, T-D	$C_{10}H_{14}N_5O_7P$	99.15	Adenosine monophosphate
3.28	267.0994	1.55	1.27E−06	D-C, T-C, T-D	$C_{10}H_{13}N_5O_4$	66.33	Adenosine
7.25	89.0468	1.54	1.27E−06	D-C, T-C, T-D	$C_3H_7NO_2$	94.58	beta-Alanine
25.08	330.255	1.54	1.51E−06	D-C, T-C, T-D	$C_{22}H_{34}O_2$	76.84	Docosapentaenoic acid (DPA)
12.79	173.1059	1.54	2.58E−06	D-C, T-C, T-D	$C_8H_{15}NO_3$	86.99	N-Acetylisoleucine
14.39	172.1103	1.54	1.27E−06	D-C, T-C, T-D	$C_9H_{16}O_3$	99.9	9-oxo-nonanoic acid
5.43	327.1332	1.53	2.58E−06	D-C, T-C, T-D	$C_{15}H_{21}NO_7$	97.34	N-(1-Deoxy-1-fructosyl)phenylalanine
2.23	343.1256	1.53	1.90E−06	D-C, T-C, T-D	$C_{15}H_{21}NO_8$	70.01	N-(1-Deoxy-1-fructosyl)tyrosine
2.38	181.0721	1.53	2.84E−06	D-C, T-C, T-D	$C_9H_{11}NO_3$	70.05	L-Tyrosine
2.64	293.1509	1.52	2.08E−06	D-C, T-C, T-D	$C_{12}H_{23}NO_7$	70.28	N-(1-Deoxy-1-fructosyl)leucine/N-(1-Deoxy-1-fructosyl)isoleucine
1.53	541.0576	1.52	6.47E−09	T-C, T-D	$C_{15}H_{21}N_5O_{13}P_2$	91.89	Cyclic ADP-ribose
22.67	521.3481	1.51	7.83E−07	T-C, T-D	$C_{26}H_{52}NO_7P$	89.79	LysoPC(18:1)
5.42	237.1027	1.51	5.48E−06	D-C, T-C, T-D	$C_{12}H_{15}NO_4$	97.49	N-lactoyl-phenylalanine
2.64	203.1178	1.41	2.08E−06	T-C, T-D	$C_9H_{17}NO_4$	91.58	N-lactoyl-Leucine
2.39	131.095	1.50	5.78E−06	D-C, T-C, T-D	$C_6H_{13}NO_2$	76.63	Beta-Leucine
9.72	366.1447	1.50	7.72E−06	D-C, T-C, T-D	$C_{17}H_{22}N_2O_7$	84.06	N-(1-Deoxy-1-fructosyl)tryptophan
22.67	507.3321	1.50	9.84E−07	T-C, T-D	$C_{25}H_{50}NO_7P$	94.44	LysoPE(20:1)
6.41	284.0768	1.50	5.87E−06	D-C, T-C, T-D	$C_{10}H_{12}N_4O_6$	89.96	Xanthosine
7.25	219.1161	1.50	7.49E−06	D-C, T-C, T-D	$C_9H_{17}NO_5$	82.88	Pantothenic acid
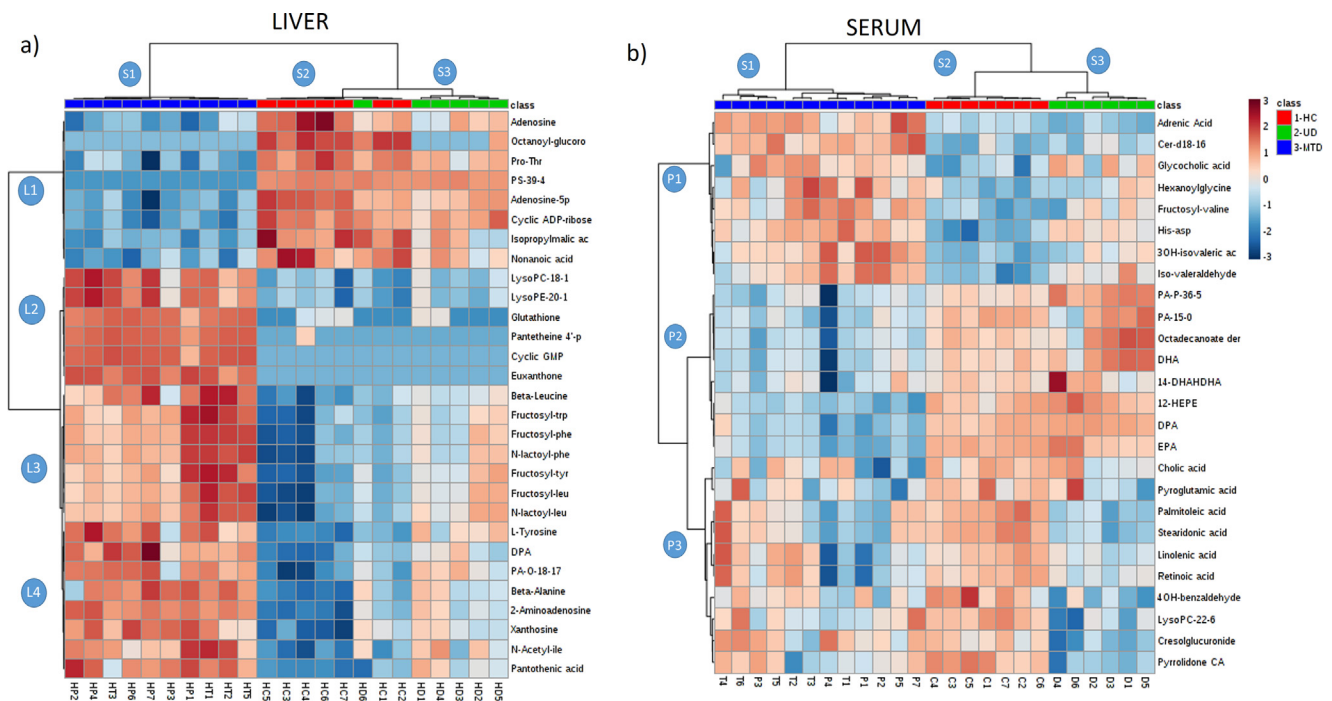
Fig. 3. Hierarchical clustering via heatmap using Pearson as distance measure and Ward as clustering algorithm, of the significant annotated metabolites. (a: liver model; b: serum model).

4.1.1. Euxanthone

Euxanthone was only detected and positively identified in the mango-treated group (L2). Mango contains numerous bioactive; however, the only metabolite that bioaccumulated/biotransformed in the liver was euxanthone. This substance is a metabolite from mangiferin, a bioactive compound found in mango and mangosteen (*Garcinia mangostana* Linn.) (Pedraza-Chaverri, Cárdenas-Rodríguez, Orozco-Ibarra, & Pérez-Rojas, 2008). When mangiferin is orally consumed, intestinal bacteria first deglycosylate it to norathyriol, leaving the core phenolic scaffolding intact (Sanugul et al., 2005). Norathyriol is then further metabolized into euxanthone by removing two hydroxyl groups at positions 3 and 6 (Derese, Guantai, Yaouba, & Kuete, 2017). Mangiferin and its metabolites are of high interest due to numerous health-promoting effects documented, such as antioxidant, anti-inflammatory, antidiabetic and others (Martin & He, 2009).

It has been shown that mangiferin is able to modulate different signaling molecules, including mitogen-activated protein kinases (MAPKs), nuclear factor kappa-light-chain-enhancer of activated B cells (NF-κB) and protein kinase C (PKC) isoforms (Saha, Sadhukhan, & Sil, 2016), the latter related to the non-enzymatic formation of advanced glycation end products (AGEs) in hyperglycemic organisms (Das Evcimen & King, 2007). Additionally, mangiferin suppresses some pro-inflammatory cytokines (Saha et al., 2016) and inhibits enzymes associated with carbohydrate metabolism, such as α-amylase and α-glucosidase (Sekar, Chakraborty, Mani, Sali, & Vasanthi, 2019), thereby exerting beneficial effects in STZ-induced diabetic rats (Gondi & Rao, 2015).

Our results suggest that euxanthone is bioaccumulated in the liver of diabetic rats after consuming a diet rich in 'Ataulfo' mango peel and pulp for five weeks, possibly contributing to the antidiabetic effects of this diet.

4.1.2. Glutathione

Glutathione was found at higher concentration in the liver of MTD rats, as compared to HC and UD animals. This finding suggests that mango consumption exerted a profound antioxidant effect by stimulating the endogenous antioxidant system. Oxidative stress in diabetic

organisms is well documented and correlates strongly with diabetic complications in most affected organs (Tangvarasittichai, 2015). Various authors have found a protective effect of phenolic-rich foods or extracts. For example, *Arafat et al.*, (Arafat et al., 2016) administered *Momordica charantia* fruit pulp to alloxan-induced diabetic rats, and found a restored hepatic glutathione concentration. Abdel-Moneim, Yousef, Abd El-Twab, Abdel Reheim, & Ashour (2017) report that gallic acid and *p*-coumaric acid (both present in mango pulp) prevent brain glutathione depletion in STZ-induced diabetic rats. Finally, it has been shown that a mangiferin pretreatment increases glutathione levels and enhances the activity of glutathione-related enzymes in cardiac tissue of rats (Prabhu, Jainu, Sabitha, & Devi, 2006), which could be related to the findings of the present work. Therefore, our data suggests that mango supplementation apparently prevents glutathione depletion in livers of diabetic rats. This is likely due to the many phenolic compounds present in 'Ataulfo' mango peel (mangiferin) and pulp (gallic acid, chlorogenic acid, protocatechuic acid and vanillic acid), which countered some of the pro-oxidative effects of diabetes.

4.2. Metabolic changes related to molecular pathophysiological mechanisms of diabetes

In addition to increased hyperglycemia, the UD group had a significantly lower weight gain than the HC and MTD groups. Induction with STZ caused a perceptible weight loss from the first week explained by the depletion of muscle and adipose tissue. However, the consumption of mango-supplemented diet resulted in substantial improvement in weight gain and the maintenance of glucose during the trial (Table S1). Particularly, changes in serum and liver metabolites were mainly related to alterations of fatty acids, bile acids, amino acids, pantothenate, and nucleotide metabolism. The above-mentioned changes are consistent with some known disrupted mechanisms linked to DM and its complications in STZ-induced rat models.

4.2.1. Fatty acid metabolism

Most changes documented in serum were related to fatty acids, their metabolites and phospholipids, indicating that lipid metabolism was

significantly altered. Interestingly, changes were found on mono-unsaturated fatty acids (MUFAs) and polyunsaturated fatty acids (PUFAs).

Palmitoleic acid decreased in both diabetic groups, as compared to the control. This MUFA is a lipokine that can promote peripheral insulin sensitivity in muscle cells via p-38 MAPK signaling (Talbot, Wheeler-Jones, & Cleasby, 2014), and in animal models by up-regulating the expression of carbohydrate- and lipid-catabolizing genes (Duckett, Volpi-Lagreca, Alende, & Long, 2014). Furthermore, linolenic acid and stearidonic acid were also significantly altered, with a decreasing tendency in both diabetic groups, while the concentration of eicosapentaenoic acid (EPA) was lower in the MTD group. These ω-3 fatty acids have shown bioactivities related to insulin resistance, and their consumption has been explored and suggested to be useful in type 2 diabetes (Jovanovski, Li, Thanh Ho, Djedovic, & Marques, 2017).

Adrenic acid, docosapentaenoic acid (DPA), docosahexaenoic acid (DHA) and 14-(docosahexaenoyloxy) docosahexaenoic acid (14-DHADHA) also showed significant changes. Increased levels of adrenic acid have been correlated with decreased insulin sensitivity and with increased area under the glucose curve in a type 2 diabetic male population (Lankinen et al., 2015). The effects of DHA have been shown to oppose those of previously-mentioned ω-6 fatty acids, for example, dietary supplementation with ω-3 fatty acids (including DHA) can improve some endocrine and anthropometric parameters in a type-2 diabetic population (Jacobo-Cejudo et al., 2017). In addition, branched fatty acid esters of hydroxy fatty acids (FAHFAs) such as 14-DHADHA has been reported to exert anti-inflammatory and anti-diabetic properties, mainly in type 2 diabetes in humans and rats (Balas, Durand, & Feillet-Coudray, 2018).

Taken together, these results showed an increased level of pro-inflammatory ω-6, concurrent with a decreased level of anti-inflammatory ω-3 fatty acids. An increased ω-6-to-ω-3 ratio has been correlated with cardiac events (Takahashi et al., 2017), suggesting that dietary supplementation of ω-3 could be beneficial in diabetic organisms.

In addition to free fatty acids, phospholipids [PA(P-36:5), PA(15:0/0:0), LPC(22:6)] and sphingolipids [ceramide (d18:1/16:0)] were also significantly altered in serum of diabetic rats. The behavior of these compounds (Fig. 3) suggests that phospholipase activity increased in the absence of insulin (Lin et al., 2016). This fact has also been found to be related to oxidative stress (Yui et al., 2015). Both phospholipids and sphingolipids are key metabolic mediators that modulate intracellular signaling related to insulin, as well as numerous other processes, which makes them important targets to prevent, mitigate or revert metabolic anomalies (Meikle & Summers, 2017).

4.2.2. Bile acids

Significant changes were documented on the serum concentration of cholic acid and glycocholic acid. The upregulation of glycocholic acid has been considered a circulating metabolomic biomarker of the disease. The regulation of hepatic bile acid metabolism has been linked to a possible prevention of insulin resistance, as observed in previous studies. In fact, a role as a ligand of the farnesoid X receptor (FXR), also known as bile acid receptor, has been assigned to bile acids (Cipriani, Mencarelli, Palladino, & Fiorucci, 2010; Renga, Mencarelli, Vavassori, Brancaleone, & Fiorucci, 2010). FXR is a transcription factor that, among other functions, stimulates insulin transcription and secretion from pancreatic β-cells.

4.2.3. Branched-chain amino acids (BCAAs) and aromatic amino acids metabolism

Main changes in liver amino acids were related to branched and aromatic amino acids. BCAAs and some of their derivatives like leucine, N-(1-deoxy-1-fructosyl)-leucine, N-lactoyl-leucine and N-(1-deoxy-1-fructosyl)-isoleucine were all increased in the liver of diabetic groups (UD and MTD), whereas, N-(1-deoxy-1-fructosyl)-valine was increased

in serum, demonstrating an impaired amino acid metabolic control, as revealed in one-week STZ-induced diabetic rats (Diao et al., 2014).

It is well known that STZ-diabetic induced rats are susceptible to increased protein catabolism in tissues like skeletal muscle, which leads to an alteration in diverse amino acid metabolic pathways, increasing circulating BCAA levels (Rodríguez et al., 1997). Since the liver is one of the principal tissues where BCAA oxidation takes place (60–83%), it is possible that excess of α-ketoacids produced from BCAA in muscles by proteolysis in diabetic organisms, is metabolized here and modulated by the branched-chain α-keto acid dehydrogenase complex (BCKDH) in this organ. This BCKDH complex would lead to the formation of acetyl-CoA or succinyl-CoA, which can enter the tricarboxylic acid cycle (TCA); once there, they can be converted into pyruvate or any gluconeogenic TCA intermediate (Neinast et al., 2019). However, hepatic BCKDH activity has been shown to decrease in diabetic rat models (Doisaki et al., 2010; Kuzuya et al., 2008), which could increase hepatic BCAA concentration. We also found a significant increase in alanine levels (tentatively produced by BCAA transamination with pyruvate), which is related to the glucose-alanine cycle from muscle to the liver, which apparently supplies gluconeogenic substrates due to a lack of inhibitory insulin signaling (Suhre et al., 2010).

Finally, our results show the upregulation of three aromatic amino acids or its fructosyl derivatives (phenylalanine, tyrosine, and tryptophan) in both diabetic groups (UD and MTD), which is consistent with data reported by *Lanza et al.* (Lanza et al., 2010). Changes in aromatic amino acids have been associated with perturbations in gut microbiota (Neis, Dejong, & Rensen, 2015), which has been reported as altered in patients with impaired glucose metabolism (Chen et al., 2016). In diabetic organisms, AGEs are formed when reducing sugars (such as glucose and fructose) spontaneously react with proteins, which has been linked to the development of diabetic neuropathy, nephropathy and retinopathy, among other complications (Karachalias, Babaei-Jadidi, Ahmed, & Thornalley, 2003).

As the concentration of fructose in serum is much lower than that of glucose, this molecule has not been a central focus on glycation research. However, it is more reactive than glucose, and has been reported to be elevated via polyol pathway activation in diabetic tissues (Gallagher, LeRoith, Stasinopoulos, Zelenko, & Shiloach, 2016).

Non-enzymatic reactions between reducing sugars and amines depend on their circulating levels, promoting the spontaneous formation of early glycation products (EGPs), including N-terminal fructosyl compounds, which are precursors of AGEs (Beisswenger, 2012). As seen in cluster L3 of the heatmap, our results show that all BCAAs and aromatic amino acids in liver and serum of diabetic rats (UD and MTD) were glycated with fructosamine residues (L3). The AGE levels and N-fructosyl-lysine were described to be increased in retinal, renal glomeruli, sciatic nerve and serum proteins in STZ-induced diabetic rats, which was related to high glycemia (Karachalias, Babaei-Jadidi, Rabbani, & Thornalley, 2010). In a previous study, increased glycated hemoglobin (HbA$_1$ = 17.7 ± 1.6%) was associated with the presence of N-fructosyl-valine in diabetic rats after a 24-week period (Karachalias et al., 2003). We can argue that in organisms with altered glucose homeostasis, glycation reactions of amino acids and other molecules increase, causing protein dysfunction and disruption of amino acid metabolism.

4.2.4. Pantothenate and CoA biosynthesis

According to our results, different precursors of CoA showed changes between groups. Pantothenic acid levels were higher in the liver of both diabetic groups, as compared to the control (L4), while pantetheine 4″-phosphate was upregulated in the MTD group (L2), suggesting an increased synthesis of CoA with predicted impact on acetyl-CoA production. An increased generation of acetyl-CoA is linked to excessive fatty acid oxidation in the liver of fasted and diabetic rats (due to the lack of carbohydrate utilization), which are metabolized in TCA or HMG-CoA pathways to produce ATP or ketone bodies,

respectively (McGarry & Foster, 1980; Wieland, Weiss, & Eger-Neufeldt, 1964).

4.2.5. Nucleotide metabolism

This study showed a decreased in adenine and AMP concentrations in the liver of both diabetic groups (UD and MTD), while there was an increase of 2-aminoadenosine and xanthosine in the liver of both diabetic groups, as compared to the HC (L1, and L4, respectively). Meanwhile, cGMP was upregulated in the MTD group (L2).

Nucleotides play a pivotal role in most metabolic pathways, acting as part of nucleic acids, coenzymes and signaling molecules. It has been reported that adenosine, AMP, guanosine, GMP, GTP, inosine and IMP are increased in type 1 and type 2 diabetes (Dudzinska, 2014; Huang et al., 2011). Increased nucleoside levels could be a result of an accelerated nucleotide degradation under diabetic conditions, changes in the enzymes and transporters responsible for their metabolism, and alterations at the genetic level (Dudzinska, 2014). Xanthosine elevation could suggest an accelerated breakdown of the xanthine in purine metabolism, which is associated with oxidative stress in the liver of diabetic rats (Kristal, Vigneau-Callahan, Moskowitz, & Matson, 1999). Regarding the increased cGMP in MTD group, the effect of phenolic compounds on the prevention and treatment of cardiovascular diseases and hypertension has been described, which are linked to stimulating endothelial nitric oxide (NO) and vasorelaxation via cGMP pathway (Benito et al., 2002). cGMP is a second messenger that promotes glucose-stimulated insulin secretion, prevents β-cells apoptosis and promote its differentiation, however, modulation of guanosine metabolites remains unclear in diabetic organisms.

5. Conclusions

The present study identified potential biomarkers related to diabetic disorders involving significant changes to fatty acid, amino acid, bile acid, pantothenate and nucleotide pathways. Furthermore, the metabolomic approach used found two main hepatic metabolites (euxanthone and glutathione) linked to mango-based dietary intervention, suggesting that some bioactive compounds present therein are bioavailable and can reach target tissues such as the liver. These findings also demonstrated that 'Ataulfo' mango consumption improves the antioxidant status of diabetic rats. Results may contribute to a better understanding of the metabolic changes that take place in diabetic organisms, and the effects of bioactive compounds from mango in STZ-induced diabetic rats. Nonetheless, further research is still needed in order to verify or refute the associations of the possible bioactivity of phenolic compounds in other altered animal tissues or in a nutritional intervention in humans.

Ethics statement

All experiments involving living organisms were reviewed and approved by the Bioethics Committee of the Research Center for Food and Development, where they were performed (CE/013/2018). Animals were cared for and manipulated according to applicable local and international rules and regulations, such as the Guide for the Care and Use of Laboratory Animals of the National Institutes of Health and the Mexican NOM-062-ZOO-1999.

CRediT authorship contribution statement

Álvaro Fernández-Ochoa: Investigation, Methodology, Writing - original draft, Software. **Rosario Cázares-Camacho:** Investigation, Methodology, Writing - original draft, Software. **Isabel Borrás-Linares:** Writing - review & editing, Supervision. **J. Abraham Domínguez-Avila:** Writing - review & editing, Supervision. **Antonio Segura-Carretero:** Conceptualization, Supervision, Project administration. **Gustavo Adolfo González-Aguilar:** Conceptualization, Supervision,

Project administration.

Declaration of Competing Interest

The authors declared that there is no conflict of interest.

Appendix A. Supplementary material

Supplementary data to this article can be found online at https://doi.org/10.1016/j.jff.2019.103695.

References

Abdel-Moneim, A., Yousef, A. I., Abd El-Twab, S. M., Abdel Reheim, E. S., & Ashour, M. B. (2017). Gallic acid and p-coumaric acid attenuate type 2 diabetes-induced neurodegeneration in rats. *Metabolic Brain Disease, 32*(4), 1279–1286. https://doi.org/10.1007/s11011-017-0039-8.

Agin, A., Heintz, D., Ruhland, E., Chao de la Barca, J. M., Zumsteg, J., Moal, V., ... Namer, I. J. (2016). Metabolomics - an overview. From basic principles to potential biomarkers (part 1). *Medecine Nucleaire, 40*, 4–10. https://doi.org/10.1016/j.mednuc.2015.12.006.

Arafat, S. Y., Nayeem, M., Jahan, S., Karim, Z., Reza, H. M., Hossain, M. H., ... Alam, M. A. (2016). Ellagic acid rich Momordica charantia fruit pulp supplementation prevented oxidative stress, fibrosis and inflammation in liver of alloxan induced diabetic rats. *Oriental Pharmacy and Experimental Medicine, 16*(4), 267–278. https://doi.org/10.1007/s13596-016-0242-x.

Balas, L., Durand, T., & Feillet-Coudray, C. (2018). Branched FAHFAs, appealing beneficial endogenous fat against obesity and type-2 diabetes. *Chemistry - A European Journal, 24*(38), 9463–9476. https://doi.org/10.1002/chem.201800853.

Beidokhti, M. N., & Jäger, A. K. (2017). Review of antidiabetic fruits, vegetables, beverages, oils and spices commonly consumed in the diet. *Journal of Ethnopharmacology, 201*, 26–41. https://doi.org/10.1016/j.jep.2017.02.031.

Beisswenger, P. J. (2012). Glycation and biomarkers of vascular complications of diabetes. *Amino Acids, 42*, 1171–1183. https://doi.org/10.1007/s00726-010-0784-z.

Benito, S., Lopez, D., Sáiz, M. P., Buxaderas, S., Sánchez, J., Puig-Parellada, P., & Mitjavila, M. T. (2002). A flavonoid-rich diet increases nitric oxide production in rat aorta. *British Journal of Pharmacology, 135*(4), 910–916. https://doi.org/10.1038/sj.bjp.0704534.

Chen, K. H., Cheng, M. L., Jing, Y. H., Chiu, D. T. Y., Shiao, M. S., & Chen, J. K. (2011). Resveratrol ameliorates metabolic disorders and muscle wasting in streptozotocin-induced diabetic rats. *American Journal of Physiology - Endocrinology and Metabolism, 301*(5), https://doi.org/10.1152/ajpendo.00048.2011.

Chen, T., Zheng, X., Ma, X., Bao, Y., Ni, Y., Hu, C., ... Jia, W. (2016). Tryptophan predicts the risk for future type 2 diabetes. *PLoS ONE, 11*(9), e0162192. https://doi.org/10.1371/journal.pone.0162192.

Cho, N. H., Shaw, J. E., Karuranga, S., Huang, Y., da Rocha Fernandes, J. D., Ohlrogge, A. W., & Malanda, B. (2018). IDF Diabetes Atlas: Global estimates of diabetes prevalence for 2017 and projections for 2045. *Diabetes Research and Clinical Practice, 138*, 271–281.

Chong, J., Soufan, O., Li, C., Caraus, I., Li, S., Bourque, G., ... Xia, J. (2018). MetaboAnalyst 4.0: Towards more transparent and integrative metabolomics analysis. *Nucleic Acids Research, 46*(W1), W486–W494. https://doi.org/10.1093/nar/gky310.

Cipriani, S., Mencarelli, A., Palladino, G., & Fiorucci, S. (2010). FXR activation reverses insulin resistance and lipid abnormalities and protects against liver steatosis in Zucker (fa / fa) obese rats. *Journal of Lipid Research, 51*(4), 771–784. https://doi.org/10.1194/jlr.m001602.

Das Evcimen, N., & King, G. L. (2007). June). The role of protein kinase C activation and the vascular complications of diabetes. *Pharmacological Research, 55*, 498–510. https://doi.org/10.1016/j.phrs.2007.04.016.

Derese, S., Guantai, E. M., Yaouba, S., & Kuete, V. (2017). Mangifera indica L. (Anacardiaceae). In Medicinal Spices and Vegetables from Africa: Therapeutic Potential Against Metabolic, Inflammatory, Infectious and Systemic Diseases (pp. 451–483). 10.1016/B978-0-12-809286-6.00021-2.

Diao, C., Zhao, L., Guan, M., Zheng, Y., Chen, M., Yang, Y., ... Gao, H. (2014). Systemic and characteristic metabolites in the serum of streptozotocin-induced diabetic rats at different stages as revealed by a ^{1}H-NMR based metabonomic approach. *Mol. BioSyst. 10*(3), 686–693. https://doi.org/10.1039/C3MB70609E.

Doisaki, M., Katano, Y., Nakano, I., Hirooka, Y., Itoh, A., Ishigami, M., ... Shimomura, Y. (2010). Regulation of hepatic branched-chain α-keto acid dehydrogenase kinase in a

rat model for type 2 diabetes mellitus at different stages of the disease. *Biochemical and Biophysical Research Communications, 393*(2), 303–307. https://doi.org/10.1016/j.bbrc.2010.02.004.

Duckett, S. K., Volpi-Lagreca, G., Alende, M., & Long, N. M. (2014). Palmitoleic acid reduces intramuscular lipid and restores insulin sensitivity in obese sheep. *Diabetes, Metabolic Syndrome and Obesity: Targets and Therapy, 7*, 553–563. https://doi.org/10.2147/DMSO.S72695.

Dudzinska, W. (2014). Purine nucleotides and their metabolites in patients with type 1 and 2 diabetes mellitus. *Journal of Biomedical Science and Engineering, 07*(01), 38–44. https://doi.org/10.4236/jbise.2014.71006.

Fernández-Ochoa, Á., Quirantes-Piné, R., Borrás-Linares, I., Gemperline, D., Alarcón Riquelme, M. E., Beretta, L., & Segura-Carretero, A. (2019). Urinary and plasma metabolite differences detected by HPLC-ESI-QTOF-MS in systemic sclerosis patients. *Journal of Pharmaceutical and Biomedical Analysis, 162*, 82–90. https://doi.org/10.1016/j.jpba.2018.09.021.

Gallagher, E. J., LeRoith, D., Stasinopoulos, M., Zelenko, Z., & Shiloach, J. (2016). Polyol accumulation in muscle and liver in a mouse model of type 2 diabetes. *Journal of Diabetes and Its Complications, 30*(6), 999–1007. https://doi.org/10.1016/j.jdiacomp.2016.04.019.

Gandhi, G. R., Jothi, G., Antony, P. J., Balakrishna, K., Paulraj, M. G., Ignacimuthu, S., ... Al-Dhabi, N. A. (2014). Gallic acid attenuates high-fat diet fed-streptozotocin-induced insulin resistance via partial agonism of PPARγ in experimental type 2 diabetic rats and enhances glucose uptake through translocation and activation of GLUT4 in PI3K/p-Akt signaling pathway. *European Journal of Pharmacology, 745*, 201–216.

Gil de la Fuente, A., Grace Armitage, E., Otero, A., Barbas, C., & Godzien, J. (2017). Differentiating signals to make biological sense – A guide through databases for MS-based non-targeted metabolomics. *Electrophoresis, 38*(18), 2242–2256. https://doi.org/10.1002/elps.201700070.

Gondi, M., & Rao, U. J. S. P. (2015). Ethanol extract of mango (Mangifera indica L.) peel inhibits α-amylase and α-glucosidase activities, and ameliorates diabetes related biochemical parameters in streptozotocin (STZ)-induced diabetic rats. *Journal of Food Science and Technology, 52*(12), 7883–7893.

Goyal, R., & Jialal, I. (2018). *Diabetes mellitus, type 2. StatPearls [Internet]*. StatPearls Publishing.

Huang, Q., Yin, P., Wang, J., Chen, J., Kong, H., Lu, X., & Xu, G. (2011). Method for liver tissue metabolic profiling study and its application in type 2 diabetic rats based on ultra performance liquid chromatography-mass spectrometry. *Journal of Chromatography B: Analytical Technologies in the Biomedical and Life Sciences, 879*(13–14), 961–967. https://doi.org/10.1016/j.jchromb.2011.03.009.

Jacobo-Cejudo, M. G., Valdés-Ramos, R., Guadarrama-López, A. L., Pardo-Morales, R. V., Martínez-Carrillo, B. E., & Harbige, L. S. (2017). Effect of n-3 polyunsaturated fatty acid supplementation on metabolic and inflammatory biomarkers in type 2 diabetes mellitus patients. *Nutrients, 9*(6), 1–11. https://doi.org/10.3390/nu9060573.

Jovanovski, E., Li, D., Thanh Ho, H. V., Djedovic, V., De Castro Ruiz Marques, A., Shishtar, E., ... Vuksan, V. (2017, May). The effect of alpha-linolenic acid on glycemic control in individuals with type 2 diabetes. Medicine (United States), Vol. 96, p. e6531. 10.1097/MD.0000000000006531.

Karachalias, N., Babaei-Jadidi, R., Ahmed, N., & Thornalley, P. J. (2003). Accumulation of fructosyl-lysine and advanced glycation end products in the kidney, retina and peripheral nerve of streptozotocin-induced diabetic rats. *Biochemical Society Transactions, 31*(6), 1423–1425. https://doi.org/10.1042/bst0311423.

Karachalias, N., Babaei-Jadidi, R., Rabbani, N., & Thornalley, P. J. (2010). Increased protein damage in renal glomeruli, retina, nerve, plasma and urine and its prevention by thiamine and benfotiamine therapy in a rat model of diabetes. *Diabetologia, 53*(7), 1506–1516. https://doi.org/10.1007/s00125-010-1722-z.

King, A., & Bowe, J. (2016). Animal models for diabetes: Understanding the pathogenesis and finding new treatments. *Biochemical Pharmacology, 99*, 1–10. https://doi.org/10.1016/j.bcp.2015.08.108.

Kristal, B. S., Vigneau-Callahan, K. E., Moskowitz, A. J., & Matson, W. R. (1999). Purine catabolism: Links to mitochondrial respiration and antioxidant defenses? *Archives of Biochemistry and Biophysics, 370*(1), 22–33. https://doi.org/10.1006/abbi.1999.1387.

Kuzuya, T., Katano, Y., Nakano, I., Hirooka, Y., Itoh, A., Ishigami, M., ... Shimomura, Y. (2008). Regulation of branched-chain amino acid catabolism in rat models for spontaneous type 2 diabetes mellitus. *Biochemical and Biophysical Research Communications, 373*(1), 94–98. https://doi.org/10.1016/j.bbrc.2008.05.167.

Lankinen, M. A., Stančáková, A., Uusitupa, M., Ågren, J., Pihlajamäki, J., Kuusisto, J., ... Laakso, M. (2015). Plasma fatty acids as predictors of glycaemia and type 2 diabetes. *Diabetologia, 58*(11), 2533–2544. https://doi.org/10.1007/s00125-015-3730-5.

Lanza, I. R., Zhang, S., Ward, L. E., Karakelides, H., Raftery, D., & Sreekumaran Nair, K. (2010). Quantitative metabolomics by 1H-NMR and LC-MS/MS confirms altered metabolic pathways in diabetes. *PLoS ONE, 5*(5), e10538. https://doi.org/10.1371/journal.pone.0010538.

Lin, X. H., Xu, M. T., Tang, J. Y., Mai, L. F., Wang, X. Y., Ren, M., & Yan, L. (2016). Effect of intensive insulin treatment on plasma levels of lipoprotein-associated phospholipase A2 and secretory phospholipase A2 in patients with newly diagnosed type 2 diabetes. *Lipids in Health and Disease, 15*(1), 1–10. https://doi.org/10.1186/s12944-016-0368-3.

Martin, M., & He, Q. (2009). Mango bioactive compounds and related nutraceutical properties-A review. *Food Reviews International, 25*, 346–370. https://doi.org/10.1080/87559120903153524.

McGarry, J. D., & Foster, D. W. (1980). Regulation of hepatic fatty acid oxidation and ketone body production. *Annual Review of Biochemistry, 49*(1), 395–420. https://doi.org/10.1146/annurev.bi.49.070180.002143.

Meikle, P. J., & Summers, S. A. (2017). Sphingolipids and phospholipids in insulin resistance and related metabolic disorders. *Nature Reviews Endocrinology, 13*, 79–91.

https://doi.org/10.1038/nrendo.2016.169.

Naveen, J., & Baskaran, V. (2018). Antidiabetic plant-derived nutraceuticals: A critical review. *European Journal of Nutrition, 57*(4), 1275–1299.

Neinast, M. D., Jang, C., Hui, S., Murashige, D. S., Chu, Q., Morscher, R. J., ... Arany, Z. (2019). Quantitative analysis of the whole-body metabolic fate of branched-chain amino acids. *Cell Metabolism, 29*(2), 417–429.e4. https://doi.org/10.1016/j.cmet.2018.10.013.

Neis, E. P. J. G., Dejong, C. H. C., & Rensen, S. S. (2015). The role of microbial amino acid metabolism in host metabolism. *Nutrients, 7*, 2930–2946. https://doi.org/10.3390/nu7042930.

Pacheco-Ordaz, R., Antunes-Ricardo, M., Gutiérrez-Uribe, J. A., & González-Aguilar, G. A. (2018). Intestinal permeability and cellular antioxidant activity of phenolic compounds from mango (Mangifera indica cv. ataulfo) peels. *International Journal of Molecular Sciences, 19*(2), https://doi.org/10.3390/ijms19020514.

Palafox-Carlos, H., Yahia, E. M., & González-Aguilar, G. A. (2012). Identification and quantification of major phenolic compounds from mango (Mangifera indica, cv. Ataulfo) fruit by HPLC–DAD–MS/MS-ESI and their individual contribution to the antioxidant activity during ripening. *Food Chemistry, 135*(1), 105–111. https://doi.org/10.1016/J.FOODCHEM.2012.04.103.

Pedraza-Chaverri, J., Cárdenas-Rodríguez, N., Orozco-Ibarra, M., & Pérez-Rojas, J. M. (2008, October). Medicinal properties of mangosteen (Garcinia mangostana). *Food and Chemical Toxicology, 46*, 3227–3239. https://doi.org/10.1016/j.fct.2008.07.024.

Prabhu, S., Jainu, M., Sabitha, K. E., & Devi, C. S. S. (2006). Role of mangiferin on biochemical alterations and antioxidant status in isoproterenol-induced myocardial infarction in rats. *Journal of Ethnopharmacology, 107*(1), 126–133. https://doi.org/10.1016/j.jep.2006.02.014.

Quirós-Sauceda, A. E., Oliver Chen, C. Y., Blumberg, J. B., Astiazaran-Garcia, H., Wall-Medrano, A., & González-Aguilar, G. A. (2017). Processing 'ataulfo' mango into juice preserves the bioavailability and antioxidant capacity of its phenolic compounds. *Nutrients, 9*(10), 1–12. https://doi.org/10.3390/nu9101082.

Renga, B., Mencarelli, A., Vavassori, P., Brancaleone, V., & Fiorucci, S. (2010). The bile acid sensor FXR regulates insulin transcription and secretion. *Biochimica et Biophysica Acta - Molecular Basis of Disease, 1802*(3), 363–372. https://doi.org/10.1016/j.bbadis.2010.01.002.

Rodríguez, T., Alvarez, B., Busquets, S., Carbó, N., López-Soriano, F. J., & Argilés, J. M. (1997). The increased skeletal muscle protein turnover of the streptozotozin diabetic rat is associated with high concentrations of branched-chain amino acids. *Biochemical and Molecular Medicine, 61*(1), 87–94. https://doi.org/10.1006/bmme.1997.2585.

Saha, S., Sadhukhan, P., & Sil, P. C. (2016). Mangiferin: A xanthonoid with multipotent anti-inflammatory potential. *BioFactors, 42*, 459–474. https://doi.org/10.1002/biof.1292.

Sanugul, K., Akao, T., Li, Y., Kakiuchi, N., Nakamura, N., & Hattori, M. (2005). Isolation of a Human Intestinal Bacterium That Transforms Mangiferin to Norathyriol and Inducibility of the Enzyme That Cleaves a C-Glucosyl Bond. *Biological & Pharmaceutical Bulletin, 28*(9), 1672–1678. https://doi.org/10.1248/bpb.28.1672.

Sas, K. M., Karnovsky, A., Michailidis, G., & Pennathur, S. (2015). Metabolomics and diabetes: Analytical and computational approaches. *Diabetes, 64*(3), 718–732. https://doi.org/10.2337/db14-0509.

Sekar, V., Chakraborty, S., Mani, S., Sali, V. K., & Vasanthi, H. R. (2019). Mangiferin from Mangifera indica fruits reduces post-prandial glucose level by inhibiting α-glucosidase and α-amylase activity. *South African Journal of Botany, 120*, 129–134.

Sellamuthu, P. S., Arulselvan, P., Muniappan, B. P., Fakurazi, S., & Kandasamy, M. (2013). Mangiferin from Salacia chinensis prevents oxidative stress and protects pancreatic β-cells in streptozotocin-induced diabetic rats. *Journal of Medicinal Food, 16*(8), 719–727.

Suhre, K., Meisinger, C., Döring, A., Altmaier, E., Belcredi, P., Gieger, C., ... Illig, T. (2010). Metabolic footprint of diabetes: A multiplatform metabolomics study in an epidemiological setting. *PLoS ONE, 5*(11), e13953. https://doi.org/10.1371/journal.pone.0013953.

Sumner, L. W., Amberg, A., Barrett, D., Beale, M. H., Beger, R., Daykin, C. A., ... Viant, M. R. (2007). Proposed minimum reporting standards for chemical analysis: Chemical Analysis Working Group (CAWG) Metabolomics Standards Initiative (MSI). *Metabolomics, 3*(3), 211–221. https://doi.org/10.1007/s11306-007-0082-2.

Szkudelski, T., & Szkudelska, K. (2015). Resveratrol and diabetes: From animal to human studies. *Biochimica et Biophysica Acta - Molecular Basis of Disease, 1852*, 1145–1154. https://doi.org/10.1016/j.bbadis.2014.10.013.

Takahashi, M., Ando, J., Shimada, K., Nishizaki, Y., Tani, S., Ogawa, T., ... Komuro, I. (2017). The ratio of serum n-3 to n-6 polyunsaturated fatty acids is associated with diabetes mellitus in patients with prior myocardial infarction: A multicenter cross-sectional study. *BMC Cardiovascular Disorders, 17*(1), 41. https://doi.org/10.1186/s12872-017-0479-4.

Talbot, N. A., Wheeler-Jones, C. P., & Cleasby, M. E. (2014). Palmitoleic acid prevents palmitic acid-induced macrophage activation and consequent p38 MAPK-mediated skeletal muscle insulin resistance. *Molecular and Cellular Endocrinology, 393*(1–2), 129–142. https://doi.org/10.1016/j.mce.2014.06.010.

Tangvarasittichai, S. (2015). Oxidative stress, insulin resistance, dyslipidemia and type 2 diabetes mellitus. *World Journal of Diabetes, 6*(3), 456. https://doi.org/10.4239/wjd.v6.i3.456.

Ulaszewska, M. M., Weinert, C. H., Trimigno, A., Portmann, R., Andres Lacueva, C., Badertscher, R., ... Vergères, G. (2019). Nutrimetabolomics: An integrative action for metabolomic analyses in human nutritional studies. *Molecular Nutrition & Food Research, 63*(1), 1800384. https://doi.org/10.1002/mnfr.201800384.

Velderrain-Rodríguez, G., Torres-Moreno, H., Villegas-Ochoa, M., Ayala-Zavala, J., Robles-Zepeda, R., Wall-Medrano, A., & González-Aguilar, G. (2018). Gallic acid content and an antioxidant mechanism are responsible for the antiproliferative activity of 'Ataulfo'mango peel on LS180 cells. *Molecules, 23*(3), 695.

Wells, A., Barrington, W. T., Dearth, S., May, A., Threadgill, D. W., Campagna, S. R., & Voy, B. H. (2018). Tissue level diet and sex-by-diet interactions reveal unique metabolite and clustering profiles using untargeted liquid chromatography-mass spectrometry on adipose, skeletal muscle, and liver tissue in C57BL6/J Mice. *Journal of Proteome Research, 17*(3), 1077–1090. https://doi.org/10.1021/acs.jproteome.7b00750.

Wieland, O., Weiss, L., & Eger-Neufeldt, I. (1964). Enzymatic regulation of liver acetyl-CoA metabolism in relation to ketogenesis. *Advances in Enzyme Regulation, 2*(C), 85–99. https://doi.org/10.1016/S0065-2571(64)80007-8.

Yui, D., Nishida, Y., Nishina, T., Mogushi, K., Tajiri, M., Ishibashi, S., ... Yokota, T. (2015). Enhanced phospholipase A2 group 3 expression by oxidative stress decreases the insulin-degrading enzyme. *PLoS ONE, 10*(12), e0143518. https://doi.org/10.1371/journal.pone.0143518.